The Journal of Immunology

Quantifying and Imaging NY-ESO-1/LAGE-1-Derived Epitopes on Tumor Cells Using High Affinity T Cell Receptors

Marco A. Purbhoo, Deborah H. Sutton, Joanna E. Brewer, Rebecca E. Mullings, Maxine E. Hill, Tara M. Mahon, Julia Karbach, Elke Jäger, Brian J. Cameron, Nikolai Lissin, Paresh Vyas, Ji-Li Chen, Vincenzo Cerundolo and Bent K. Jakobsen

J Immunol 2006; 176:7308-7316; ;
doi: 10.4049/jimmunol.176.12.7308
http://www.jimmunol.org/content/176/12/7308

The Journal of Immunology is published twice each month by
The American Association of Immunologists, Inc.,
1451 Rockville Pike, Suite 650, Rockville, MD 20852

Print ISSN: 0022-1767 Online ISSN: 1550-6606.

Quantifying and Imaging NY-ESO-1/LAGE-1-Derived Epitopes on Tumor Cells Using High Affinity T Cell Receptors

Marco A. Purbhoo,* Deborah H. Sutton,* Joanna E. Brewer,* Rebecca E. Mullings,* Maxine E. Hill,* Tara M. Mahon,* Julia Karbach,† Elke Jäger,† Brian J. Cameron,* Nikolai Lissin,* Paresh Vyas,‡ Ji-Li Chen,§ Vincenzo Cerundolo,§ and Bent K. Jakobsen[1]*

Presentation of intracellular tumor-associated Ags (TAAs) in the context of HLA class I molecules offers unique cancer-specific cell surface markers for the identification and targeting of tumor cells. For most peptide Ags, the levels of and variations in cell surface presentation remain unknown, yet these parameters are of crucial importance when considering specific TAAs as targets for anticancer therapy. Here we use a soluble TCR with picomolar affinity for the HLA-A2-restricted 157–165 epitope of the NY-ESO-1 and LAGE-1 TAAs to investigate presentation of this immunodominant epitope on the surface of a variety of cancer cells. By single molecule fluorescence microscopy, we directly visualize HLA-peptide presentation for the first time, demonstrating that NY-ESO-1/LAGE-1-positive tumor cells present 10–50 NY-ESO-1/LAGE-$1_{157–165}$ epitopes per cell. ***The Journal of Immunology,*** **2006, 176: 7308–7316.**

Human tumors overexpress a variety of tumor-associated Ags (TAAs),[2] which are either absent or expressed at low levels in normal tissues. Peptides derived from TAAs are presented on the surface of tumor cells by class I HLA molecules and represent targets for cytotoxic or immunotherapeutic anticancer agents. The highly homologous NY-ESO-1 and LAGE-1 proteins are germ cell Ags of unknown function, which are frequently expressed in a variety of tumors including melanoma, breast cancer (1) and, most prominently, myeloma (2). NY-ESO-1 and LAGE-1 are highly immunogenic, and CTL responses to an immunodominant, HLA-A2-restricted NY-ESO-1/LAGE-$1_{157–165}$ epitope (SLLMWITQC) can commonly be detected in cancer patients (3, 4). There has thus been a major focus on NY-ESO-1/LAGE-1 as candidates for the development of immunotherapeutic cancer vaccination (5–8).

A great unknown in the study of Ag presentation is the precise amount of any particular Ag displayed on the surface of an APC. Because the majority of HLAs are complexed to peptides derived from the most abundant cellular proteins, such as ribosomal or heat shock proteins (9), it is likely that less abundant cellular proteins, such as NY-ESO-1 or LAGE-1, are presented only at low levels. Certain TAAs may thus not be efficiently Ag presented, suggesting that there is a need to quantify the abundance of particular peptide-HLA Ags to assess the validity of specific TAAs as targets for anticancer immunotherapy. To date, the number of specific peptide-HLA complexes has been estimated mainly by mass spectroscopy of Ags eluted from cell surface HLA (10–14). HLA class I-associated Ags have also been detected on cells using Abs (15–17) or Fab monomers/tetramers (18–20) specific for given peptide-HLA complexes, allowing semiquantitative determination of surface Ag levels by FACS. A similar approach has used soluble monomers (21, 22), dimers (23), or tetramers (24, 25) of soluble TCRs to detect class I-restricted Ags, although given the naturally low affinity of TCR for Ag, it remains uncertain how quantitative and Ag sensitive such measurements are.

We have recently described the phage display-based affinity maturation of two HLA-A2-restricted soluble TCRs (26), the first specific for the $Tax_{11–19}$ epitope of HTLV-1 (isolated from CTL clone A6; Ref. 27) and the second (isolated from CTL clone 1G4; Ref. 28) specific for the NY-ESO-$1_{157–165}$ epitope. Affinity maturation of the $Tax_{11–19}$-specific TCR resulted in a 720-fold increase in affinity of TCR for Ag (from 1.8 μM to 2.5 nM), whereas a 224,000-fold increase in affinity (from 11 μM to 49 pM; Table I) was achieved for the NY-ESO-$1_{157–165}$-specific TCR, without apparent loss of Ag specificity. High affinity soluble TCRs have obvious uses in the treatment of disease, such as drug targeting or blocking of Ag-specific immune responses, which would not be possible using wild-type TCRs due to their low Ag affinities. Given their high specificity and stable interaction with Ag, such high affinity TCRs may also be useful tools in diagnostic or research contexts. Here we investigate the ability of our high affinity TCR to stain cell surface Ag, and, by single-molecule microscopy, directly determine the number of specific NY-ESO-$1_{157–165}$ Ags presented on the surface of peptide-pulsed cells, tumor cell lines, and freshly isolated tumor samples.

Materials and Methods

Soluble protein production and affinity measurements

Protein production. Soluble high affinity TCRs were produced as disulfide-linked $\alpha\beta$ heterodimers, as previously described (26, 29). In the TCR-bio constructs, the TCR β-chain was C-terminally extended to encode the optimized biotinylation sequence GSGGGLNDIFEAQKIEWH. Tagged TCR was biotinylated with BirA biotin ligase (Avidity) according to the manufacturer's instruction. In the TCR-IL2 fusion constructs, the mature human IL-2 protein was fused to the C terminus of the TCR β-chain via a linker of amino acid sequence PG.

*Avidex, Ltd., Abingdon, United Kingdom; †II. Medizinische Klinik, Hämatologie-Onkologie, Krankenhaus Nordwest, Frankfurt, Germany; ‡ and ‡Medical Research Council Molecular Haematology Unit and §Tumor Immunology Unit, Weatherall Institute of Molecular Medicine, John Radcliffe Hospital, University of Oxford, Oxford, United Kingdom

Received for publication November 18, 2005. Accepted for publication April 5, 2006.

The costs of publication of this article were defrayed in part by the payment of page charges. This article must therefore be hereby marked *advertisement* in accordance with 18 U.S.C. Section 1734 solely to indicate this fact.

[1] Address correspondence and reprint requests to Dr. Bent Jakobsen, Avidex, Ltd., 57c Milton Park, Abingdon OX14 4RX, United Kingdom. E-mail address: bent.jakobsen@avidex.com

[2] Abbreviations used in this paper: TAA, tumor-associated Ag; SPR, surface plasmon resonance.

0022-1767/06/$02.00

Table I. *Wild-type and high affinity TCR specific for HLA-A2 complexed NY-ESO-1$_{157–165}$*[a]

Clone	CDR2α	CDR3α	CDR2β	TCRβF3	CDR3β	K_d 9C (nM)	K_d 9V (nM)
WT	IQSSQ	PTSGGSYIPT	GAGI	QGEVPNGYNVSRSTT	YVGN	11,700	5,500
113	I**TPW**Q	P**LLDG**TYIPT	**AIQT**	**R**GEVPNGYNVSRST**I**	Y**L**GN	0.049	0.038

[a] Summary of sequence and kinetic data for wild-type and high affinity NYE(113) TCRs. Amino acid sequences are in single letter code. Sequence changes to wild type in the high affinity TCR variant are shown in bold. TCR affinities for NY-ESO-1$_{157–165}$/HLA-A2 Ag were determined for both the wild-type (9C) and 9V variant peptide by SPR.

Surface plasmon resonance (SPR). We conducted Biacore SPR analysis of TCR binding to biotin-tagged HLA-A2/SLLMWITQ(C/V), immobilized to a streptavidin-coated flow cell. Equilibrium binding constants for TCRs exhibiting slow off-rates were calculated from kinetic data ($K_D = k_{off}/k_{on}$). Kinetic binding constants were calculated via Biacore BIAevaluation software, using all available data except for points up to ~25 s after the injection starts and points within ~10 s of injection stops. Dissociate phase data were collected for at least 45 min to allow accurate determination of the extremely slow k_{off} values.

Cells and transfections

Cells. HCT116, Colo205 *Sca*BER, PP, J82, TCCSUP, and T2 cell lines were from the American Type Culture Collection. Mel-526 and Mel-624 melanoma cells were from Thymed. SK-Mel-37 melanoma cells were from the Ludwig Institute of Cancer Research. Cells were maintained in R-10 medium (RPMI 1640 with 10% FCS, 2 mM L-glutamine, and penicillin plus streptomycin). Where indicated, cells were treated with 1000 U/ml human IFN-γ (Preprotech) for 72 h. Cancer cells were screened for NY-ESO-1 and LAGE-1 expression by RT-PCR as previously described (30). CTL were cultured in Iscove's medium (Life Technologies) supplemented with 5% human serum (TCS Biologicals), 2 mM L-glutamine, and penicillin plus streptomycin. CTL (10^5) were restimulated every 2 wk using a mixture of peptide-pulsed, irradiated (3000 rad) HLA-A2-positive PBMC (5×10^6) and peptide-pulsed cells (5×10^5). 1 μg/ml PHA (Sigma-Aldrich) and 200 U/ml Proleukin (Chiron) were added during restimulation. Proleukin was replenished every 3–4 days. Cells were used in experiments 10 days after restimulation.

Tumor samples. Myeloma cells were isolated from bone marrow aspirates. Bone marrow (2 ml) was diluted 1/2 with HBSS (Life Technologies) and incubated in 0.0002% DNase (Sigma-Aldrich) for 30 min at 37°C. Cells were loaded onto Histopaque 1077 gradient (Sigma-Aldrich) and spun at 2000 rpm ($800 \times g$) with brake off for 30 min. Cells were washed four times with HBSS, and $CD138^+$ cells were purified by magnetic separation using a $CD138^+$ MACS separation kit (Miltenyi Biotec). Cells were stained by FACS for HLA-A2 and NY-ESO-1 expression. All work on human tumor samples was approved by Oxford Research Ethics Committee B.

SLLMWITQC-minigene transfectants. The SLLMWITQC epitope was expressed as a C-terminal fusion to the third ubiquitin subunit of human polyubiquitin. The ubiquitin subunit was amplified by PCR from cDNA derived from human bladder carcinoma cell line TCCSUP. The SLLMWITQC epitope was fused to ubiquitin by PCR, with the 3′ primer used in this amplification lacking the ubiquitin C-terminal Cysteine and stop codons, but encoding the (human-codon optimized) epitope sequence followed by a TAG stop codon. The fusion construct was ligated into the first multiple cloning site of pIRES (Clontech), whereas the Blasticidin resistance gene from vector pEM7/bsd (Invitrogen Life Technologies) was inserted into the second multiple cloning site of pIRES. Transfectants were selected in the presence of 10 μg/ml Blasticidin (Invitrogen Life Technologies).

Cellular assays

Cytokine assays. For the IFN-γ ELISPOT assays (Diaclone), 500 CTL were added to 5×10^4 target cells/well. TCR was added to 5 μg/ml. Assays were left overnight at 37°C and developed according to manufacturer's instructions. Plates were evaluated using an automated ELISPOT reader (Autoimmun Diagnostika). For the IFN-γ release assays (Diaclone), 1.5×10^4 peptide-pulsed T2 target cells per well were incubated with TCR at 37°C for 1 h before addition of 5×10^3 CTL. Assays were left for 48 h at 37°C. IFN-γ concentration in supernatant was determined according to manufacturer's instructions. Data were analyzed using Prism 4.0 software (Graphpad Software).

FACS. For staining with high affinity TCR, 10^6 T2 cells were pulsed with peptide for 90 min at 37°C and washed twice with PBS. Cells were stained with 10 μg/ml monomeric TCR-IL2 or TCR-bio in 1% FCS/PBS for 30 min at room temperature, followed by two washes in 10 ml of PBS. Secondary staining was in 1% FCS-PBS for 30 min at room temperature with PE-linked rat anti-human IL-2 mAb (Serotec) or streptavidin-PE (BD Pharmingen), respectively. Cells were washed twice in PBS and analyzed by FACS. Cell surface HLA-A2 levels were determined by FACS using FITC-linked mouse anti-HLA-A2 mAb (Serotec). For intracellular NY-ESO-1 detection by FACS, cells were permeabilized with 70% ethanol on ice for 30 min and stained with NY-ESO-1-specific mAb E978 (Zymed) followed by PE-linked F(ab′)2 rabbit anti-mouse secondary Ab (Serotec).

Immunohistochemistry. Cells (10^7) were pelleted, resuspended in 100 μl of a 1:1 medium-OCT mixture, and snap frozen. Cryostat sections (5–8 μm) were cut, placed on Superfrost plus slides, and dried at room temperature. Slides were fixed in acetone for 10 min and air dried. Slides were submerged in water, mounted onto the Sequenza apparatus, and washed in TBS (pH 7.8). Slides were blocked for 30 min in 10% v/v normal rabbit serum (Vector Laboratories), and stained with mTCR-bio followed by streptavidin-biotin-HRP complex (DAKO). Diaminobenzidine (DakoCytomation liquid and substrate chromagen system) was added according to manufacturer's instructions and counterstained with hematoxylin. Finally, slides were dehydrated, cleared, and mounted.

Microscopy

A Zeiss 200M/Universal Imaging system with a ×63 objective was used for single-molecule wide field fluorescence microscopy and data analysis as described (31, 32). Eight-well chambered coverslips (Nunc) with minimal imaging medium (R-10 lacking phenol red) were used for imaging.

For Ag staining with high affinity TCR, 5×10^4 cancer cells were allowed to adhere to chambered coverslips overnight. Cells were washed twice with PBS supplemented with 400 nM $MgCl_2$ and 400 nM $CaCl_2$ ($PBS_{Mg/Ca}$), and incubated for 30 min at room temperature with 5 μg/ml TCR-bio in 0.5% BSA/$PBS_{Mg/Ca}$. Cells were washed three times with $PBS_{Mg/Ca}$ and incubated for 20 min at room temperature with 5 μg/ml streptavidin-PE in 0.5% BSA/$PBS_{Mg/Ca}$. Cells were washed five times, and chamber wells were filled with 400 μl of imaging medium. For washed, peptide-pulsed T2 cells, staining with TCR-bio and streptavidin PE was essentially as for adherent cells above, except that cells were washed once with 10 ml of PBS between the primary and secondary stains and twice with 10 ml of PBS after the secondary stain.

PE fluorescence was detected using a 535/50 excitation, 610/75 emission, and 565LP dichroic filter set (Chroma). Given that staining of cell surface-bound biotinylated complexes with an excess of streptavidin-PE has been shown to result in monomeric association of streptavidin-PE with target protein (31, 32), a single detected PE signal corresponds to a single TCR-peptide-HLA complex. To cover the entire three-dimensional surface of the cell, *z*-stack fluorescent images were taken (21 individual planes, 1 μm apart). Data were evaluated for at least 20 cells in each experimental condition.

Results

Detection of Ag on target cells

We have previously shown by SPR that the interaction between our high affinity NYE(113) TCR and its Ag is extraordinarily stable, with the half-life of the interaction estimated at 19 h (26). To determine the ability of the NYE(113) TCR to detect cell surface Ag, we investigated the stability and Ag sensitivity of TCR binding to Ag-pulsed T2 cells. We generated TCR constructs in which the TCR β-chain was C-terminally tagged with either IL-2 (TCR-IL-2) or biotinylated via a biotinylation sequence (TCR-bio). These constructs could be easily detected using a PE-linked anti-IL-2 mAb or streptavidin-PE, respectively. T2 cells were pulsed with a variant of the NY-ESO-1$_{157–165}$ peptide reported to enhance peptide association with HLA-A2 in which the C-terminal cysteine

at position 9 (9C) has been replaced with a more standard valine anchor residue (9V) (28, 33, 34). Recognition of HLA-A2-complexed peptide by high affinity NYE(113) TCR was virtually unaffected by this 9V substitution (Table I).

We observed exceptionally stable binding of NYE(113) TCR-IL-2 to Ag-pulsed T2 cells at 37°C over 6 h (Fig. 1*A*), in accordance with the long half-life of this TCR-Ag interaction as determined by SPR. In contrast, the TAX(134) TCR-IL-2 rapidly dissociated from T2 cells pulsed with cognate Ag, consistent with the significantly shorter half-life (50 min) of the TAX(134) TCR interaction with Ag (26). Both high affinity TCRs dissociated from Ag-pulsed targets ~2.5-fold more rapidly than expected from their half-lives as determined by SPR, most likely reflecting increased dissociation kinetics at 37°C (cellular staining assay) compared with 25°C (SPR). FACS analysis of T2 cells pulsed with a titration of Ag showed that staining with monomeric NYE(113) TCR-bio/streptavidin-PE was sensitive enough to detect Ag on cells pulsed with as low as 10^{-8} M peptide (Fig. 1*B*). Because the maximal sensitivity of FACS for PE is generally believed to be ~200–500 PE molecules/cell (BD Biosciences technical support), we investigated whether we could detect even lower Ag levels by single-molecule fluorescence microscopy. In this system, the entire three-dimensional cell surface is imaged to detect individual PE molecules (31, 32). Because TCR-bio/peptide/HLA complexes are labeled with streptavidin-PE in a 1:1 ratio, the number of PE molecules determined is directly representative of the number of Ags present on the cell surface. Using this highly sensitive approach, we could detect Ags at the single-digit level, even on cells pulsed with as little as 10^{-10} M peptide (Fig. 1*C*).

To investigate staining of HLAs endogenously loaded with wild-type (9C) NY-ESO-$1_{157–165}$ Ag, we transfected five HLA-A2 positive cell lines with a SLLMWITQC-minigene construct. The NY-ESO-$1_{157–165}$ epitope was expressed as a C-terminal fusion to human ubiquitin (35–37). Upon expression, this construct undergoes proteolytic cleavage at the ubiquitin/epitope junction, thus generating free, cytoplasmic epitope which can be translocated into the endoplasmic reticulum and loaded onto class I HLA. The bright staining of minigene-transfected J82 bladder carcinoma cells with NYE(113) TCR-bio monomer and streptavidin-PE revealed that considerable amounts of SLLMWITQC/HLA-A2 were being presented on the cell surface (Fig. 2*A*). Although exogenous pulsing of cells with the native (9C) NY-ESO-$1_{157–165}$ Ag results in inefficient HLA loading, most likely due to oxidation of the C-terminal cysteine (33), and thus peptide dimerization, endogenous loading of this epitope resulted in high Ag/HLA-A2 levels comparable with those observed for $Tax_{11–19}$ minigene-transfected J82 cells (data not shown). Competition with 10- or 100-fold excess of nonbiotinylated cold NYE(113) TCR (which is not detected by streptavidin-PE) during staining reduced the signal proportionally. Untransfected J82 cells showed no Ag-specific staining (data not shown). From the mean PE levels (~130/cell) determined when cold TCR was used in 100-fold excess, we calculated that minigene-transfected J82 cells express an average steady state level of ~13,000 SLLMWITQC/HLA-A2 cell surface Ags. Preincubation of cells with a 2-fold excess of cold NYE(113) TCR inhibited subsequent staining with NYE(113)-bio/streptavidin-PE (data not shown), indicating specificity of TCR binding. Ag could be detected on all five minigene-transfected cell lines by FACS, though levels varied considerably between cell lines (Fig. 2*B*), reflecting differing HLA-A2 expression levels (Fig. 2*C*). Cells were stimulated with IFN-γ to determine the effect of this cytokine on Ag presentation. NY-ESO-$1_{157–165}$ epitope presentation increased significantly (in most cases severalfold) after cells were

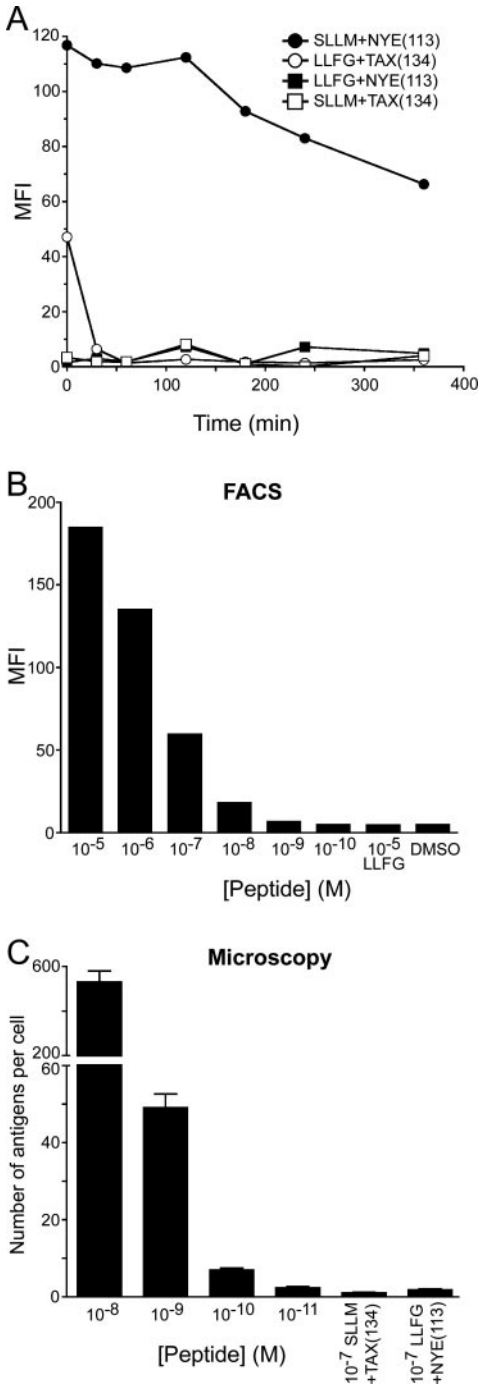

FIGURE 1. Binding of monomeric high affinity TCR to peptide-pulsed T2 cells. *A,* Stability of NYE(113) TCR-IL-2 binding to peptide-pulsed T2 cells at 37°C. Binding of NYE(113) TCR-IL-2 to T2 cells pulsed with 1 μM SLLMWITQV (●) or irrelevant HTLV-1 $Tax_{11–19}$ peptide LLFGYPVYV (■). Stability of NYE(113) TCR-IL-2 staining is compared with that of high affinity, $TAX_{11–19}$-specific TAX(134) TCR-IL-2 bound to T2 cells pulsed with LLFGYPVYV (○) or irrelevant peptide SLLMWITQV (□). *B,* FACS analysis of high affinity NYE(113) TCR-bio staining of T2 cells pulsed with a titration of SLLMWITQV peptide. Background staining levels are indicated by cells pulsed with irrelevant peptide (LLFGYPVYV) or no peptide (DMSO only). *C,* Ag levels on SLLMWITQV-pulsed T2 cells as determined by three-dimensional fluorescence microscopy. Cells were stained with NYE(113) TCR-bio/streptavidin-PE. Control stains (SLLMWITQV peptide + TAX(134) TCR-bio, or LLFGYPVYV peptide + NYE(113) TCR-bio) are shown to indicate background staining. MFI, Mean fluorescence intensity.

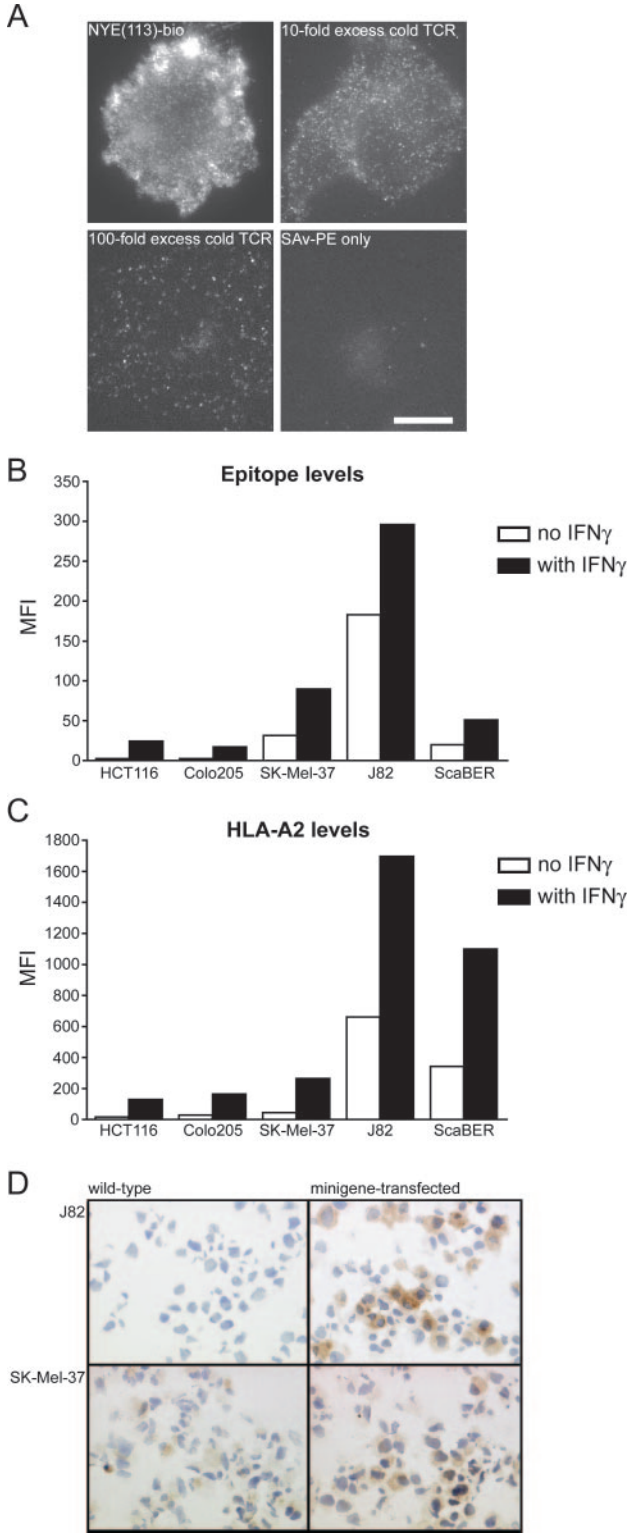

FIGURE 2. Staining of NY-ESO-$1_{157–165}$ minigene expressing cells with high affinity TCR. *A,* Imaging of individual SLLMWITQC/HLA-A2 Ags on SLLMWITQC-minigene-transfected J82 bladder carcinoma cell line. Cells were stained with high affinity NYE(113) TCR-bio monomers and streptavidin-PE. Each dot on the fluorescent images represents a single streptavidin-PE/TCR/Ag-HLA complex. Specificity of TCR-bio binding was demonstrated by costaining with a 10- or 100-fold excess of cold (nonbiotinylated) NYE(113) TCR. Three-dimensional fluorescent images of cells were acquired, although only the lower, slide-proximal surface of each cell is shown. Cells stained with streptavidin-PE only are shown as control. Cells shown are representative of the brightest 10% found among each staining condition. *Bar,* 10 μm. Levels of cell surface SLLMWITQC/HLA-A2 (*B*), or HLA-A2 complexes (*C*) were determined for each SLLMWITQC-minigene-transfected cell line by FACS, using a high affinity NYE(113) TCR or anti-HLA-A2 mAb to stain with, respectively. Where indicated, cell lines were cultured in the presence of IFN-γ. *D,* NYE(113) TCR staining of snap-frozen SLLWITQC-minigene-transfected J82 and SK-Mel-37 cells by immunohistochemistry. MFI, Mean fluorescence intensity.

treated with IFN-γ, in accordance with similar up-regulation of cell surface HLA-A2.

To determine whether our high affinity TCRs could be used to detect Ag by immunohistochemistry, we snap froze NY-ESO-$1_{157–165}$ mingene-transfected cells in a 1:1 medium-OTC mixture and stained sections with NYE(113) TCR as described. Sections of minigene-transfected J82 and SK-Mel-37 clearly stained with NYE(113) TCR (Fig. 2*D*). Wild-type SK-Mel37 cells, unlike wild-type J82 cells, express NY-ESO-1 and LAGE-1 proteins. Low level staining by immunohistochemistry was observed in untransfected SK-Mel-37 cells, but not in untransfected J82 cells, indicating that immunohistochemistry could be used to detect NY-ESO-$1_{157–165}$ Ags derived from endogenous proteins.

Inhibition of Ag-specific CTL responses by soluble high affinity TCR

CTL responses are both Ag specific and highly sensitive. To confirm the specificity of the NYE(113) TCR, we examined the ability of this TCR to inhibit IFN-γ release by NY-ESO-$1_{157–165}$-specific CTL clone 1G4 (28). CTL clone 1G4 was sensitive to T2 cells pulsed with Ag concentrations as low as 10^{-10} M (Fig. 3*A*). Half-maximal activation was observed just below 10^{-9} M Ag, corresponding to <50 Ags per APC (as determined from Fig. 1*C*). Such sensitivity is in agreement with findings that CTL require only a few (~10) Ags at the immunological synapse to become activated (31). Addition of the NYE(113) TCR inhibited 1G4 CTL activation in a dose- and Ag level-dependent manner. CTL activation could be completely inhibited by the NYE(113) TCR, indicating specific blockage of virtually every Ag/HLA complex (Fig. 3*B*). In contrast, wild-type NYE TCR was unable to inhibit 1G4 CTL responses at any concentration tested (Fig. 3*C*), indicating that masking of Ags by wild-type affinity TCR is too transient to affect CTL target recognition. Similarly, using two further NY-ESO-$1_{157–165}$-specific CTLs of different origins, inhibition of CTL-mediated target cell lysis was observed in the presence of high affinity NYE(113) TCR, but not with wild-type affinity TCR (Fig. 3*D*).

Determination of the number of NY-ESO-$1_{157–165}$ Ags presented on cancer cell lines and fresh tumor isolates

Although NY-ESO-1 and LAGE-1 expression is observed at high frequency in many cancers, it remains unknown at what levels the NY-ESO-$1_{157–165}$ Ag is presented on the cancer cell surface. Therefore, we aimed to detect and quantify NY-ESO-$1_{157–165}$ Ag on the surface of HLA-A2-positive melanoma cancer cell lines SK-Mel-37, Mel-624, and Mel-526 which have previously been reported to be recognized by SLLMWITQC-specific CTL (Refs. 38 and 39; Thymed, unpublished observation). We evaluated NY-ESO-1 and LAGE-1 expression in these cells lines by FACS and RT-PCR (Fig. 4*A*). Endogenous NY-ESO-1 protein was detected by FACS in SK-Mel-37 cells and, at low levels, in Mel-526 cells using the NY-ESO-1-specific mAb E978 (which does not cross-react with LAGE-1; Ref. 40). NY-ESO-1 expression was not detected by FACS in Mel-624 cells. RT-PCR confirmed NY-ESO-1 expression in SK-Mel-37 cells and indicated that these cells also coexpress LAGE-1. Consistent with the Ab staining, Mel-624 cells were negative for NY-ESO-1 by RT-PCR but proved positive for

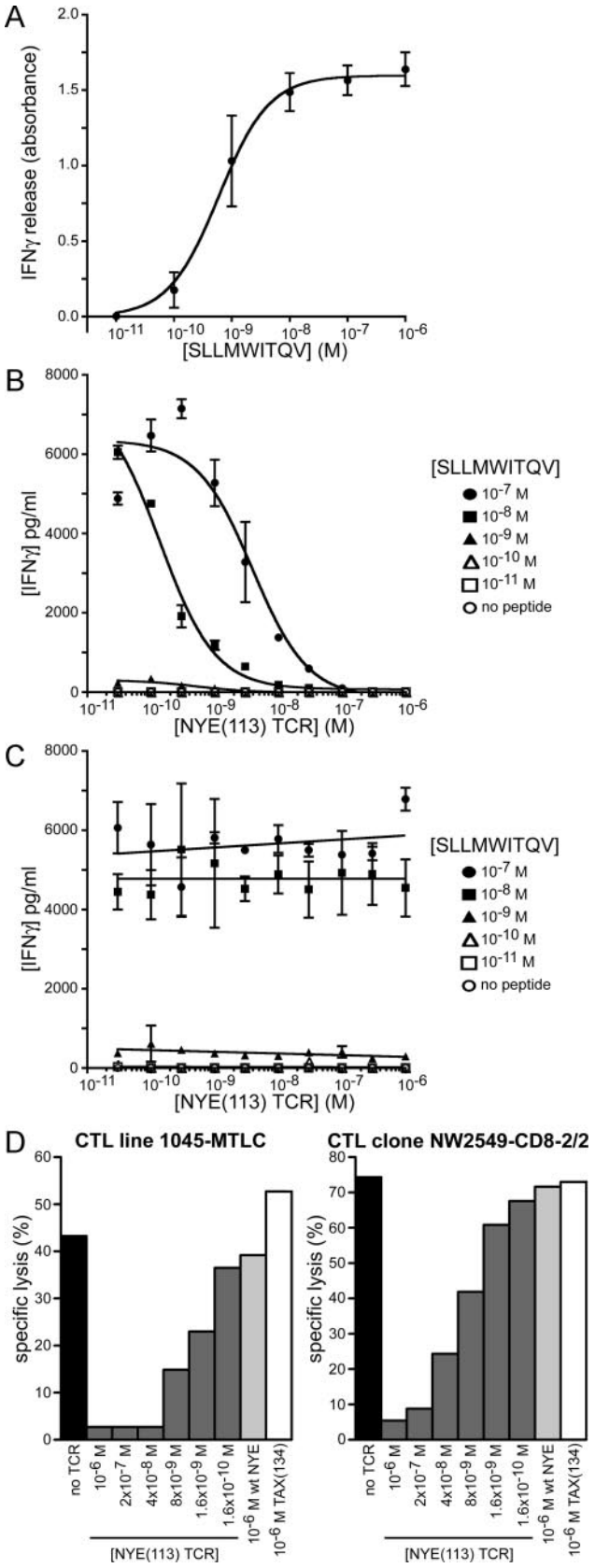

FIGURE 3. Inhibition of NY-ESO-$1_{157–165}$-specific CTL responses by high affinity TCR. *A,* IFN-γ response of NY-ESO-$1_{157–165}$-specific CTL (clone 1G4) to T2 cells pulsed with a titration of SLLMWITQV peptide. *B,* Inhibition of the CTL (clone 1G4) IFN-γ response to SLLMWITQV-pulsed T2 cells by a titration of high affinity NYE(113) TCR. Efficiency of TCR-mediated CTL inhibition was investigated at the various peptide concentrations indicated. *C,* Inhibition of the CTL (clone 1G4) IFN-γ response to SLLMWITQV-pulsed T2 cells by a titration of wild-type NYE TCR. Efficiency of TCR mediated CTL inhibition was investigated at the various peptide concentrations indicated. *D,* Inhibition of CTL-mediated lysis of T2 cells (pulsed with 10 nM SLLMWITQV) by a titration of high affinity NYE(113) TCR. Data shown are for NY-ESO-$1_{157–165}$-specific CTL line 1045-MTLC and CTL clone NW2549-CD8–2/2. Target cell lysis in the absence of TCR, in the presence of wild-type NYE TCR and in the presence of irrelevant TAX(134) TCR are shown as controls.

LAGE-1 expression. Mel-526 cells were negative for both NY-ESO-1 and LAGE-1 by RT-PCR. Although this result for Mel-526 cells appears to contrast with the positive NY-ESO-1 detection by FACS, such discrepancy between RT-PCR and staining with E978 mAb has been previously reported for cells that stain weakly with the E978 mAb (40). We next stained SK-Mel-37, Mel-624, and Mel-526 cells with NYE(113) TCR to evaluate surface presentation of the NY-ESO-$1_{157–165}$ Ag on these cell lines. We were unable to detect NY-ESO-$1_{157–165}$ cell surface Ag with NYE(113) TCR by FACS (data not shown), suggesting that Ag levels fell below the detection threshold set by flow cytometric analysis. This assumption was confirmed by single-molecule fluorescence microscopy, with which we could readily image and enumerate the number of specific Ags on individual melanoma cells (Fig. 4, *B–E*). We found that SK-Mel-37 cells presented an average of ~25 Ags per cell, whereas levels were somewhat higher for Mel-624 melanoma cells, at ~45 Ags per cell (Fig. 4, *C* and *D*). Ag counts varied broadly among individual cells, indicating the level of heterogeneity in Ag expression that may be encountered within individual tumors. Ag staining could be inhibited by a 50-fold excess of cold NYE(113) TCR, and the low background staining levels seen with irrelevant TAX(134) TCR-bio proved to be entirely due to nonspecific binding of streptavidin-PE to the cancer cell surface. For Mel-526 cells, we were unable to detect significant Ag levels, although the average NYE(113) TCR-bio staining consistently lay slightly above background in all three repeat experiments (Fig. 4*E*). This suggests that these cells may express very low levels of Ag, consistent with the low level of intracellular NY-ESO-1 as detected by FACS. Of seven HLA-A2-positive, NY-ESO-1- and LAGE-1-negative cancer cell lines, none showed specific staining with our NYE(113) TCR-bio (data not shown). The Ag levels that we determined for SK-Mel-37 and Mel-624 cells were biologically significant, given that these cells were efficiently recognized by CTL in an IFN-γ ELISPOT assay (Fig. 4, *C* and *D*). As seen previously, IFN-γ secretion in this assay could be blocked by addition of the NYE(113) TCR, but not by irrelevant TAX(134) TCR. A small amount of specific, and TCR-inhibitable, CTL activity was observed in response to Mel-526 cells (Fig. 4*E*), supporting our conclusion by FACS and microscopy that these cells do express Ag, albeit at low copy numbers. Unlike for our minigene-transfected cell lines, the presence of IFN-γ did not significantly affect Ags levels on cells that naturally express NY-ESO-1 and/or LAGE-1 (SK-Mel-37, Mel-624, and Mel-526). In contrast, IFN-γ treatment resulted in severalfold up-regulation of surface HLA-A2 (Fig. 4*F*), indicating that Ag processing, not HLA levels, is the limiting step for NY-ESO-$1_{157–165}$ presentation.

To determine whether NY-ESO-$1_{157–165}$ presentation could be detected in freshly obtained tumor samples, we isolated $CD138^+$ myeloma cells from bone marrow aspirates and stained these with NYE(113) TCR-bio/streptavidin-PE (Fig. 5). NY-ESO-1^+ myeloma ($CD138^+$) cells derived from two HLA-$A2^+$ patients (patients 1 and 2) showed specific staining with the NYE(113) TCR. In contrast, no staining was observed for $CD138^-$, nonmyeloma cells from patient 2. Furthermore, no Ag-specific staining was

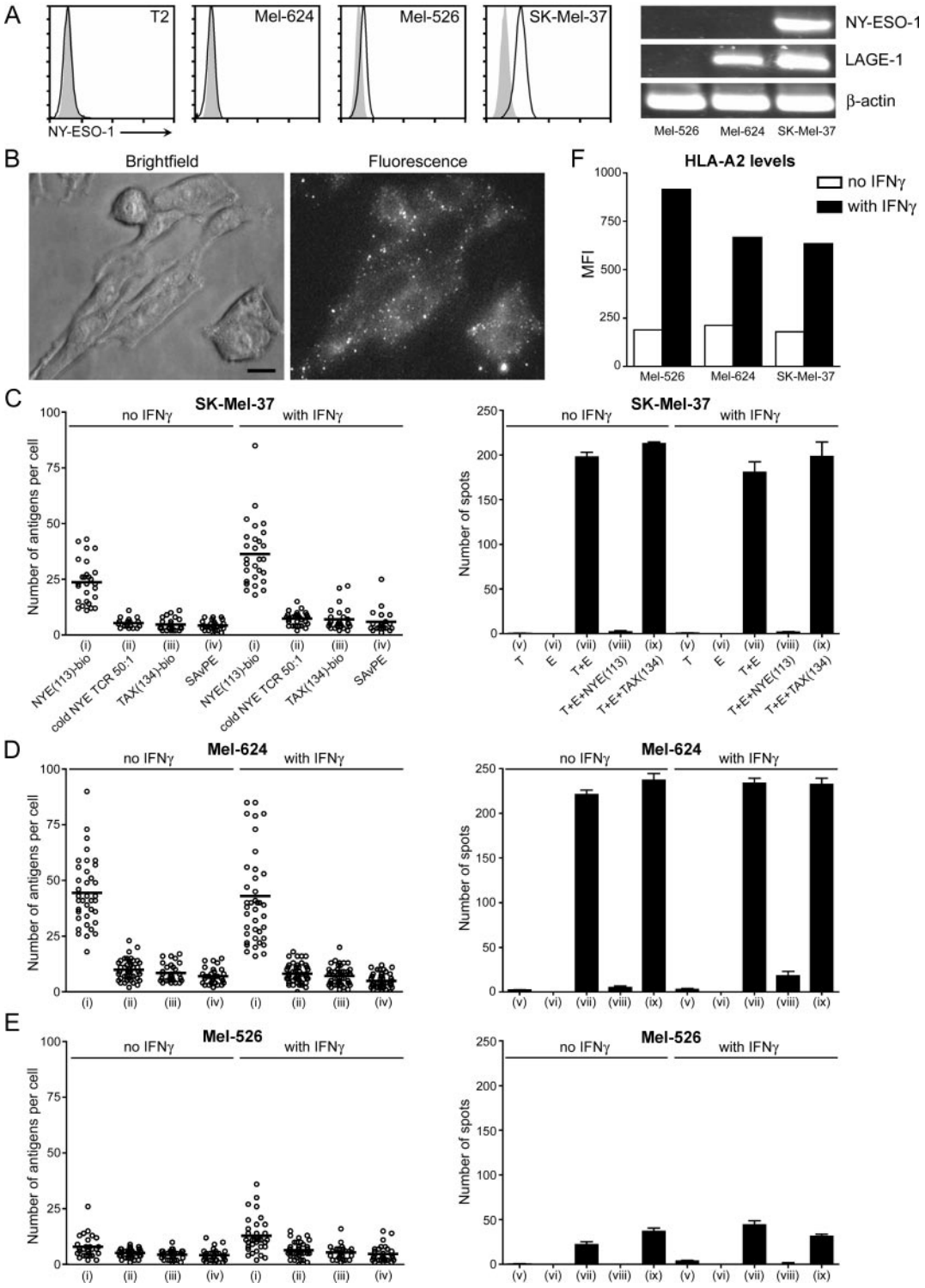

FIGURE 4. Number of NY-ESO-$1_{157–165}$ Ags presented by human cancer cells. *A,* NY-ESO-1 and LAGE-1 expression in melanoma cells. FACS plots of Mel-624, SK-Mel-37, and Mel-526 melanoma cells stained with NY-ESO-1-specific mAb E978 (bold line) or isotype control (shaded area). NY-ESO-1^- T2 cells were stained as negative control. NY-ESO-1 and LAGE-1 expression in SK-Mel-37, Mel-624, and Mel-526 cells was also determined by RT-PCR. *B–E,* Number of SLLMWITQC/HLA-A2 complexes presented by NY-ESO-1^+ melanoma cells. *B,* Imaging of total NY-ESO-$1_{157–165}$ Ag presented on Mel-624 melanoma cells. Cells were stained with high affinity NYE(113) TCR-bio monomers and streptavidin-PE. The entire three-dimensional surface of the cell was imaged by fluorescent microscopy. The fluorescent image is a maximum projection of the three-dimensional image, thus depicting the total PE count per cell. Brightfield image shows position of cell cluster. Ten cells are shown in image. *Bar,* 10 μm. *C–E,* Ag levels on individual cells were determined from three-dimensional fluorescent images of SK-Mel-37 (*C*), Mel-624 (*D*), and Mel-526 (*E*) melanoma cells stained with TCR-bio/streptavidin-PE. Each experimental condition included: (i) staining with NYE(113) TCR-bio to determine cell surface Ag levels, (ii) costaining with 50-fold excess of cold (nonbiotinylated) NYE(113) TCR to demonstrate TCR specificity, and staining with (iii) the irrelevant high affinity TAX(134)-bio(26) or (iv) streptavidin-PE alone to determine background staining levels. Vertical bars indicate mean values of the individual counts. Anti-IFN-γ ELISPOT of CTL (clone 1G4) responses were investigated for all three melanoma call lines. Each experimental condition included: (v) target cells alone (T); (vi) effector cells alone (E); (vii) targets added to effectors (T+E); (viii) targets plus effectors in the presence of NYE(113) TCR (T+E+NYE(113)); and (ix) targets and effectors in the presence of high affinity TAX(134) TCR (T+E+TAX(134)). *F,* FACS analysis of HLA-A2 levels on Mel-526, Mel-624, and SK-Mel-37 cell lines. *B–F,* Where indicated, cell lines were cultured in the presence of IFN-γ before analysis.

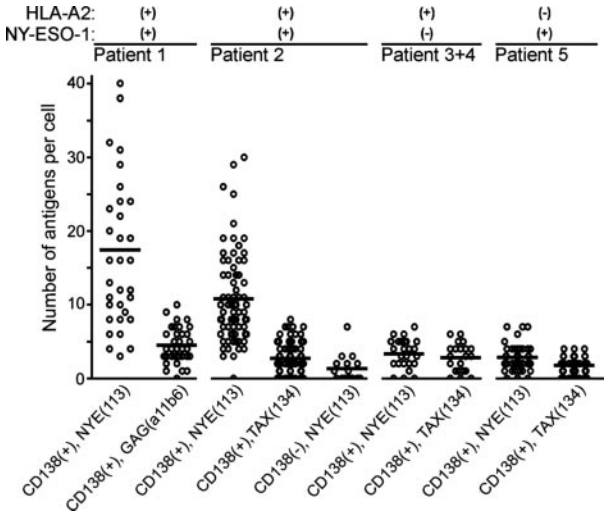

FIGURE 5. NY-ESO-$1_{157–165}$ Ag quantification on fresh myeloma isolates. Quantification of NY-ESO-$1_{157–165}$ epitopes on $CD138^+$ myeloma cells using NYE(113) TCR. As a control, cells were stained with irrelevant TCR using either the Tax(134) TCR (patients 2–5) or a high affinity TCR (clone GAGa11b6) specific for the HLA-A2-restricted $Gag_{77–85}$ epitope of HIV-1 (patient 1). Myeloma samples from patients 1 and 2 were HLA-$A2^+$ and NY-ESO-1^+. For patient 2, $CD138^-$ (nonmyeloma) cells were also stained with NYE(113) TCR. Myeloma samples from patients 3 and 4 were HLA-$A2^+$ but showed no detectable NY-ESO-1 expression, whereas the myeloma sample from patient 5 was NY-ESO-1^+ but HLA-$A2^-$.

observed on $CD138^+$ cells from two (HLA-$A2^+$) patients with NY-ESO-1^- myelomas (patients 3 and 4) or on CD138/NY-ESO-1^+ cells from a HLA-$A2^-$ patient (patient 5).

Discussion

In this study, we visualize the HLA-A2-restricted NY-ESO-$1_{157–165}$ epitope on the surface of APCs using a high affinity soluble TCR. Using such high affinity TCR, we are able to detect specific surface Ag by FACS, immunohistochemistry, and fluorescence microscopy. We show stable binding of monomeric, high affinity TCR to peptide-pulsed APCs and further correlate peptide concentration to the number of surface Ag-HLA complexes formed, demonstrating that our staining is sensitive enough to detect even single-digit numbers of Ag. We confirm Ag specificity of our high affinity TCR through its ability to inhibit NY-ESO-$1_{157–165}$-specific CTL responses and further show that this inhibitory capacity is a direct consequence of the increased affinity of our TCR for Ag, because wild-type TCR is unable to effect Ag-specific CTL responses. Finally, we directly image and enumerate the number of individual NY-ESO-$1_{157–165}$ Ags presented on malignant melanoma cancer cell lines and freshly isolated myeloma cells, giving us unique insights into the physiological surface densities of this Ag.

Current thoughts on the efficiency of Ag presentation suggest that the most abundant Ags presented are derived from the proteins with the highest rate of synthesis, such as heat shock, ribosomal, or viral proteins (41). The typical cellular protein is thus believed to be inefficiently presented, with only a few (or no) Ags reaching the cell surface. Our observation that NY-ESO-1^+ and/or LAGE-1^+ cancer cells present an average of ~10–50 NY-ESO-$1_{157–165}$ Ags per cell suggests that this density represents the physiological level at which most self Ags and TAAs are presented. This suggestion is further supported by our observation that these Ag densities are sufficient to induce effective CTL responses. Interestingly, unlike observations for our minigene-transfected cells, NY-ESO-$1_{157–165}$ Ag levels on melanoma cells were largely unaffected by IFN-γ-induced up-regulation of HLA-A2 levels, indicating that NY-ESO-1/LAGE-1 processing, and not HLA levels, is limiting in the case of this Ag. Given that tumor cells frequently express low HLA class I levels in an attempt to evade immune surveillance, it may be that the most effective anticancer immune responses are directed to those low level TAAs that are largely unaffected by HLA down-regulation.

Because the majority of cellular Ags, including TAAs, are likely to be presented at low densities, the reagents to detect these complexes are required to be highly sensitive to low numbers of Ag. Soluble binding molecules, such as TCRs, Fabs, or MHCs, are frequently oligomerized to increase binding to surface bound target molecules. However, for such oligomers (including Abs, which are natural Fab dimers), the avidity effects of multiple binding sites comes into effect only if target molecules are densely packed and more than one binding subunit can interact with its target. At low target concentrations, such as the physiological densities of most self peptide-HLA Ags on the cell surface, targets will be too sparse for an oligomer to bind multiple targets simultaneously. Thus, any interaction with low density targets will be monomeric, with the stability of the interaction determined by the affinity of the single oligomer subunit. Given the low natural affinity of TCRs for Ag, it is improbable that oligomers of wild-type TCR, even those with somewhat above average Ag affinities (21), will be able to detect low levels or quantitate high levels of Ag. In the light of our observations, it is surprising that flow cytometric staining of a HLA-$A2_{low}$ human melanoma cell line with a murine derived single-chain TCR with 2.2 μM Ag affinity indicated the presence of several thousand $p53_{264–272}$-HLA-A2 complexes per cell (21, 23), specifically because such inferred Ag levels are also difficult to reconcile with current thoughts on Ag presentation.

The affinity of the monomeric TAX(134) TCR for Ag (2.5 nM) falls within the range of Ag affinities commonly displayed by the Fab regions of Abs. Because this TCR dissociates fairly rapidly from Ag-pulsed APCs (within 30 min), nanomolar affinity reagents, including peptide-HLA specific Fabs, may not be ideal for detecting low levels of Ag. Instead, detection and quantification of physiological levels of self-Ags may require monomeric reagents with picomolar affinities, such as can be achieved by affinity-matured TCRs.

Previous studies on an affinity-maturated murine alloreactive TCR (42) have suggested that high affinity TCRs can show significant cross-reactivity to self peptides (43). We have not observed cross-reactivity of our syngenic high affinity TAX(134) and NYE(113) TCRs when tested against a broad panel of peptide-HLA complexes by SPR (26). It has been reported that the wild-type TAX TCR cross-reacts against a variety of naturally occurring epitopes that mimic the $Tax_{11–19}$ sequence (44). The binding of wild-type TAX TCR and our high affinity TAX(134) TCR to the two most cross-reactive of these mimitopes (the *Saccharomyces cereviseae* $Tel1p_{549–557}$ and *Homo sapiens* $HuD_{87–95}$ epitopes) has been previously investigated by SPR (25). Wild-type and high affinity TAX TCRs bound HLA-A2-complexed $Tel1p_{549–557}$ with similar affinities (38.6 and 46.5 μM, respectively), whereas the affinity for the $HuD_{87–95}$ epitope was increased 5-fold for the high affinity TCR (from 21 μM to 123 μM). This increase, however, is small when compared with the 720-fold increase in binding for cognate Ag, suggesting that in fact our high affinity TAX(134) TCR is comparatively less cross-reactive than the wild-type TAX TCR. For our high affinity NYE(113) TCR, we show here by single epitope imaging that only NY-ESO-1/LAGE-1-expressing or Ag-pulsed cells are stained, indicating that this TCR does not cross-react with other Ags among the cellular pool of presented self-peptides, even at the single-molecule level. We have thus

shown in a variety of biophysical and cellular assays that our high affinity TCRs are not significantly cross-reactive with self-Ags, a finding of fundamental importance when considering the development of high affinity TCRs for clinical therapies.

In summary, we aim to develop high affinity TCRs for use in immunotherapy, such as Ag-specific drug targeting, and we show here that our high affinity TCRs are capable of targeting Ag at low, physiological densities without appreciable cross-reactivity to other self-Ags. Furthermore, our observation that high affinity TCRs are able to inhibit T cell responses by stable masking of specific epitopes is a critical indicator that high affinity TCRs may also be capable of blocking specific immune responses, such as those involved in autoimmune diseases. Finally, our high affinity TCRs are shown here to be unique tools for investigating and characterizing the presentation of specific Ags, thus addressing parameters, such as Ag density, critical to the design of therapeutic approaches. Our current efforts to produce high affinity TCRs specific for numerous self or foreign Ags presented on HLA class I, HLA class II, or HLA-like molecules (26) will facilitate a wealth of comparative studies leading to a greater understanding of the cellular immune response.

Acknowledgments

We thank Malkit Sami, Penio Todorov, Neil Watson, Cornelli van der Walt, Andrew Johnson, Ruth Moysey, Emma Baston, and Annelise Vuidepot for the preparation of soluble TCRs; Andrew Millar for handling ethics approval; Jens Samol and Anna Schuhas for obtaining myeloma samples from patients; Graeme Denton at Medical Solutions for the IHC staining; and Peter Molloy, Steven Dunn, Yi Li, and Rebecca Ashfield for advice and suggestions.

Disclosures

The authors have no financial conflict of interest.

References

1. Chen, Y. T., M. J. Scanlan, U. Sahin, O. Tureci, A. O. Gure, S. Tsang, B. Williamson, E. Stockert, M. Pfreundschuh, and L. J. Old. 1997. A testicular antigen aberrantly expressed in human cancers detected by autologous antibody screening. *Proc. Natl. Acad. Sci. USA* 94: 1914–1918.
2. van Rhee, F., S. M. Szmania, F. Zhan, S. K. Gupta, M. Pomtree, P. Lin, R. B. Batchu, A. Moreno, G. Spagnoli, J. Shaughnessy, and G. Tricot. 2005. NY-ESO-1 is highly expressed in poor-prognosis multiple myeloma and induces spontaneous humoral and cellular immune responses. *Blood* 105: 3939–3944.
3. Jager, E., Y. T. Chen, J. W. Drijfhout, J. Karbach, M. Ringhoffer, D. Jager, M. Arand, H. Wada, Y. Noguchi, E. Stockert, L. J. Old, and A. Knuth. 1998. Simultaneous humoral and cellular immune response against cancer-testis antigen NY-ESO-1: definition of human histocompatibility leukocyte antigen (HLA)-A2-binding peptide epitopes. *J. Exp. Med.* 187: 265–270.
4. Valmori, D., V. Dutoit, D. Lienard, D. Rimoldi, M. J. Pittet, P. Champagne, K. Ellefsen, U. Sahin, D. Speiser, F. Lejeune, J. C. Cerottini, and P. Romero. 2000. Naturally occurring human lymphocyte antigen-A2 restricted $CD8^+$ T-cell response to the cancer testis antigen NY-ESO-1 in melanoma patients. *Cancer Res.* 60: 4499–4506.
5. Jager, E., S. Gnjatic, Y. Nagata, E. Stockert, D. Jager, J. Karbach, A. Neumann, J. Rieckenberg, Y. T. Chen, G. Ritter, et al. 2000. Induction of primary NY-ESO-1 immunity: $CD8^+$ T lymphocyte and antibody responses in peptide-vaccinated patients with NY-ESO-1^+ cancers. *Proc. Natl. Acad. Sci. USA* 97: 12198–12203.
6. Dutoit, V., R. N. Taub, K. P. Papadopoulos, S. Talbot, M. L. Keohan, M. Brehm, S. Gnjatic, P. E. Harris, B. Bisikirska, et al. 2002. Multiepitope $CD8^+$ T cell response to a NY-ESO-1 peptide vaccine results in imprecise tumor targeting. *J. Clin. Invest.* 110: 1813–1822.
7. Gnjatic, S., E. Jager, W. Chen, N. K. Altorki, M. Matsuo, S. Y. Lee, Q. Chen, Y. Nagata, D. Atanackovic, Y. T. Chen, et al. 2002. $CD8^+$ T cell responses against a dominant cryptic HLA-A2 epitope after NY-ESO-1 peptide immunization of cancer patients. *Proc. Natl. Acad. Sci. USA* 99: 11813–11818.
8. Palmowski, M. J., L. Lopes, Y. Ikeda, M. Salio, V. Cerundolo, and M. K. Collins. 2004. Intravenous injection of a lentiviral vector encoding NY-ESO-1 induces an effective CTL response. *J. Immunol.* 172: 1582–1587.
9. Jardetzky, T. S., W. S. Lane, R. A. Robinson, D. R. Madden, and D. C. Wiley. 1991. Identification of self peptides bound to purified HLA-B27. *Nature* 353: 326–329.
10. van Els, C. A., C. A. Herberts, E. van der Heeft, M. C. Poelen, J. A. van Gaans-van den Brink, A. van der Kooi, P. Hoogerhout, G. Jan ten Hove, H. D. Meiring, and A. P. de Jong. 2000. A single naturally processed measles virus peptide fully dominates the HLA-A*0201-associated peptide display and is mutated at its anchor position in persistent viral strains. *Eur. J. Immunol.* 30: 1172–1181.
11. Herberts, C. A., K. J. Stittelaar, E. van der Heeft, J. van Gaans-Van den Brink, M. C. Poelen, P. J. Roholl, L. J. van Alphen, C. J. Melief, A. P. de Jong, and C. A. van Els. 82:2131. 2001. A measles virus glycoprotein-derived human CTL epitope is abundantly presented via the proteasomal-dependent MHC class I processing pathway. *J. Gen. Virol.*
12. Wang, W., P. H. Gulden, R. A. Pierce, J. Shabanowitz, S. T. Man, D. F. Hunt, and V. H. Engelhard. 1997. A naturally processed peptide presented by HLA-A*0201 is expressed at low abundance and recognized by an alloreactive CD8+ cytotoxic T cell with apparent high affinity. *J. Immunol.* 158: 5797–5804.
13. Pascolo, S., M. Schirle, B. Guckel, T. Dumrese, S. Stumm, S. Kayser, A. Moris, D. Wallwiener, H. G. Rammensee, and S. Stevanovic. 2001. A MAGE-A1 HLA-A A*0201 epitope identified by mass spectrometry. *Cancer Res.* 61: 4072–4077.
14. Schirle, M., W. Keilholz, B. Weber, C. Gouttefangeas, T. Dumrese, H. D. Becker, S. Stevanovic, and H. G. Rammensee. 2000. Identification of tumor-associated MHC class I ligands by a novel T cell-independent approach. *Eur. J. Immunol.* 30: 2216–2225.
15. Chames, P., S. E. Hufton, P. G. Coulie, B. Uchanska-Ziegler, and H. R. Hoogenboom. 2000. Direct selection of a human antibody fragment directed against the tumor T-cell epitope HLA-A1-MAGE-A1 from a nonimmunized phage-Fab library. *Proc. Natl. Acad. Sci. USA* 97: 7969–7974.
16. Denkberg, G., C. J. Cohen, A. Lev, P. Chames, H. R. Hoogenboom, and Y. Reiter. 2002. Direct visualization of distinct T cell epitopes derived from a melanoma tumor-associated antigen by using human recombinant antibodies with MHC- restricted T cell receptor-like specificity. *Proc. Natl. Acad. Sci. USA* 99: 9421–9426.
17. Held, G., M. Matsuo, M. Epel, S. Gnjatic, G. Ritter, S. Y. Lee, T. Y. Tai, C. J. Cohen, L. J. Old, M. Pfreundschuh, Y. Reiter, H. R. Hoogenboom, and C. Renner. 2004. Dissecting cytotoxic T cell responses towards the NY-ESO-1 protein by peptide/MHC-specific antibody fragments. *Eur. J. Immunol.* 34: 2919–2929.
18. Cohen, C. J., N. Hoffmann, M. Farago, H. R. Hoogenboom, L. Eisenbach, and Y. Reiter. 2002. Direct detection and quantitation of a distinct T-cell epitope derived from tumor-specific epithelial cell-associated mucin using human recombinant antibodies endowed with the antigen-specific, major histocompatibility complex-restricted specificity of T cells. *Cancer Res.* 62: 5835–5844.
19. Cohen, C. J., G. Denkberg, A. Lev, M. Epel, and Y. Reiter. 2003. Recombinant antibodies with MHC-restricted, peptide-specific, T-cell receptor-like specificity: new tools to study antigen presentation and TCR-peptide-MHC interactions. *J. Mol. Recognit.* 16: 324–332.
20. Chang, C. C., M. Campoli, N. P. Restifo, X. Wang, and S. Ferrone. 2005. Immune selection of hot-spot β_2-microglobulin gene mutations, HLA-A2 allospecificity loss, and antigen-processing machinery component down-regulation in melanoma cells derived from recurrent metastases following immunotherapy. *J. Immunol.* 174: 1462–1471.
21. Card, K. F., S. A. Price-Schiavi, B. Liu, E. Thomson, E. Nieves, H. Belmont, J. Builes, J. A. Jiao, J. Hernandez, J. Weidanz, et al. 2004. A soluble single-chain T-cell receptor IL-2 fusion protein retains MHC-restricted peptide specificity and IL-2 bioactivity. *Cancer Immunol. Immunother.* 53: 345–357.
22. Epel, M., J. D. Ellenhorn, D. J. Diamond, and Y. Reiter. 2002. A functional recombinant single-chain T cell receptor fragment capable of selectively targeting antigen-presenting cells. *Cancer Immunol. Immunother.* 51: 565–573.
23. Mosquera, L. A., K. F. Card, S. A. Price-Schiavi, H. J. Belmont, B. Liu, J. Builes, X. Zhu, P. A. Chavaillaz, H. I. Lee, J. A. Jiao, et al. 2005. In vitro and in vivo characterization of a novel antibody-like single-chain TCR human IgG1 fusion protein. *J. Immunol.* 174: 4381–4388.
24. Subbramanian, R. A., C. Moriya, K. L. Martin, F. W. Peyerl, A. Hasegawa, A. Naoi, H. Chhay, P. Autissier, D. A. Gorgone, M. A. Lifton, et al. 2004. Engineered T-cell receptor tetramers bind MHC-peptide complexes with high affinity. *Nat. Biotechnol.* 22: 1429–1434.
25. Laugel, B., J. M. Boulter, N. Lissin, A. Vuidepot, Y. Li, E. Gostick, L. E. Crotty, D. C. Douek, J. Hemelaar, D. A. Price, B. K. Jakobsen, and A. K. Sewell. 2005. Design of soluble recombinant T cell receptors for antigen targeting and T cell inhibition. *J. Biol. Chem.* 280: 1882–1892.
26. Li, Y., R. Moysey, P. E. Molloy, A. L. Vuidepot, T. Mahon, E. Baston, S. Dunn, N. Liddy, J. Jacob, B. K. Jakobsen, and J. M. Boulter. 2005. Directed evolution of human T-cell receptors with picomolar affinities by phage display. *Nat. Biotechnol.* 23: 349–354.
27. Utz, U., D. Banks, S. Jacobson, and W. E. Biddison. 1996. Analysis of the T-cell receptor repertoire of human T-cell leukemia virus type 1 (HTLV-1) Tax-specific $CD8^+$ cytotoxic T lymphocytes from patients with HTLV-1-associated disease: evidence for oligoclonal expansion. *J. Virol.* 70: 843–851.
28. Chen, J. L., P. R. Dunbar, U. Gileadi, E. Jager, S. Gnjatic, Y. Nagata, E. Stockert, D. L. Panicali, Y. T. Chen, A. Knuth, L. J. Old, and V. Cerundolo. 2000. Identification of NY-ESO-1 peptide analogues capable of improved stimulation of tumor-reactive CTL. *J. Immunol.* 165: 948–955.
29. Boulter, J. M., M. Glick, P. T. Todorov, E. Baston, M. Sami, P. Rizkallah, and B. K. Jakobsen. 2003. Stable, soluble T-cell receptor molecules for crystallization and therapeutics. *Protein Eng.* 16: 707–711.
30. Lethe, B., S. Lucas, L. Michaux, C. De Smet, D. Godelaine, A. Serrano, E. De Plaen, and T. Boon. 1998. *LAGE-1*, a new gene with tumor specificity. *Int. J. Cancer.* 76: 903–908.
31. Purbhoo, M. A., D. J. Irvine, J. B. Huppa, and M. M. Davis. 2004. T cell killing does not require the formation of a stable mature immunological synapse. *Nat. Immunol.* 5: 524–530.

32. Irvine, D. J., M. A. Purbhoo, M. Krogsgaard, and M. M. Davis. 2002. Direct observation of ligand recognition by T cells. *Nature* 419: 845–849.
33. Bownds, S., P. Tong-On, S. A. Rosenberg, and M. Parkhurst. 2001. Induction of tumor-reactive cytotoxic T-lymphocytes using a peptide from NY-ESO-1 modified at the carboxy-terminus to enhance HLA-A2.1 binding affinity and stability in solution. *J. Immunother.* 24: 1–9.
34. Chen, J. L., G. Stewart-Jones, G. Bossi, N. M. Lissin, L. Wooldridge, E. M. Choi, G. Held, P. R. Dunbar, R. M. Esnouf, M. Sami, et al. 2005. Structural and kinetic basis for heightened immunogenicity of T cell vaccines. *J. Exp. Med.* 201: 1243–1255.
35. Bachmair, A., D. Finley, and A. Varshavsky. 1986. In vivo half-life of a protein is a function of its amino-terminal residue. *Science* 234: 179–186.
36. Johnsson, N., and A. Varshavsky. 1994. Ubiquitin-assisted dissection of protein transport across membranes. *EMBO J.* 13: 2686–2698.
37. Valmori, D., U. Gileadi, C. Servis, P. R. Dunbar, J. C. Cerottini, P. Romero, V. Cerundolo, and F. Levy. 1999. Modulation of proteasomal activity required for the generation of a cytotoxic T lymphocyte-defined peptide derived from the tumor antigen MAGE-3. *J. Exp. Med.* 189: 895–906.
38. Chen, Y. T., A. O. Gure, S. Tsang, E. Stockert, E. Jager, A. Knuth, and L. J. Old. 1998. Identification of multiple cancer/testis antigens by allogeneic antibody screening of a melanoma cell line library. *Proc. Natl. Acad. Sci. USA* 95: 6919–6923.
39. Huarte, E., J. Karbach, S. Gnjatic, A. Bender, D. Jager, M. Arand, D. Atanackovic, J. Skipper, G. Ritter, Y. T. Chen, et al. 2004. HLA-DP4 expression and immunity to NY-ESO-1: correlation and characterization of cytotoxic $CD4^+CD25^-CD8^-$ T cell clones. *Cancer Immun.* 4: 15.
40. Vaughan, H. A., S. Svobodova, D. Macgregor, S. Sturrock, A. A. Jungbluth, J. Browning, I. D. Davis, P. Parente, Y. T. Chen, E. Stockert, et al. 2004. Immunohistochemical and molecular analysis of human melanomas for expression of the human cancer-testis antigens NY-ESO-1 and LAGE-1. *Clin Cancer Res.* 10: 8396–8404.
41. Yewdell, J. W., E. Reits, and J. Neefjes. 2003. Making sense of mass destruction: quantitating MHC class I antigen presentation. *Nat. Rev. Immunol.* 3: 952–961.
42. Holler, P. D., P. O. Holman, E. V. Shusta, S. O'Herrin, K. D. Wittrup, and D. M. Kranz. 2000. In vitro evolution of a T cell receptor with high affinity for peptide/MHC. *Proc. Natl. Acad. Sci. USA* 97: 5387–5392.
43. Holler, P. D., L. K. Chlewicki, and D. M. Kranz. 2003. TCRs with high affinity for foreign pMHC show self-reactivity. *Nat. Immunol.* 4: 55–62.
44. Hausmann, S., W. E. Biddison, K. J. Smith, Y. H. Ding, D. N. Garboczi, U. Utz, D. C. Wiley, and K. W. Wucherpfennig. 1999. Peptide recognition by two HLA-A2/Tax11–19-specific T cell clones in relationship to their MHC/peptide/TCR crystal structures. *J. Immunol.* 162: 5389–5397. Vol. 176 No. 12